Amorphous alloys

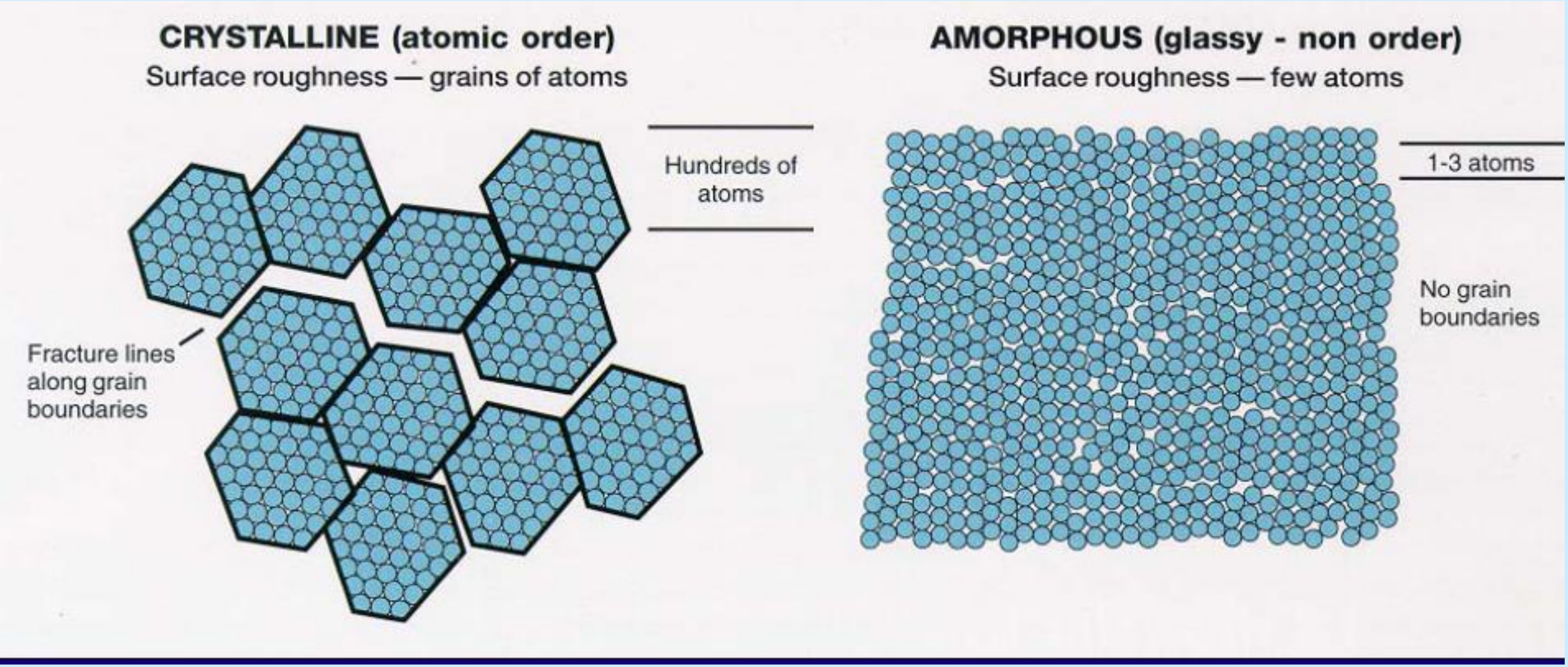

Atomic Long Range Order
(Crystal Lattice)

Short Range Order 1 - 2 nm
(Frozen Liquid)

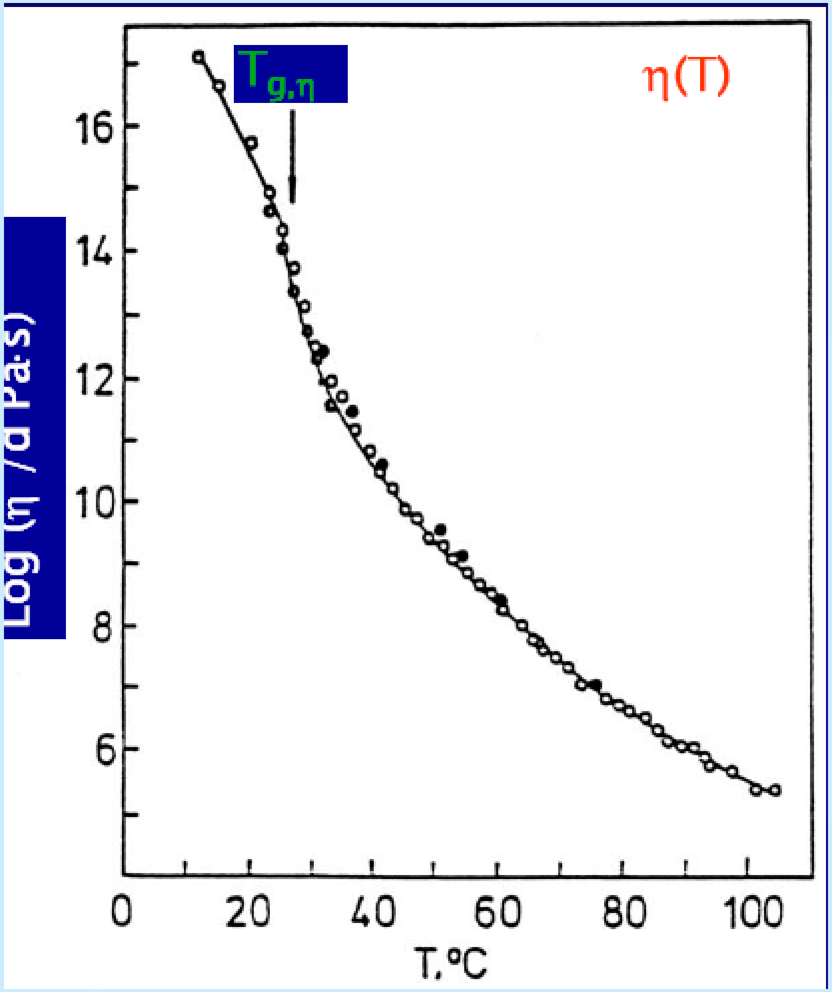

Temperature dependence of the viscosity of Se

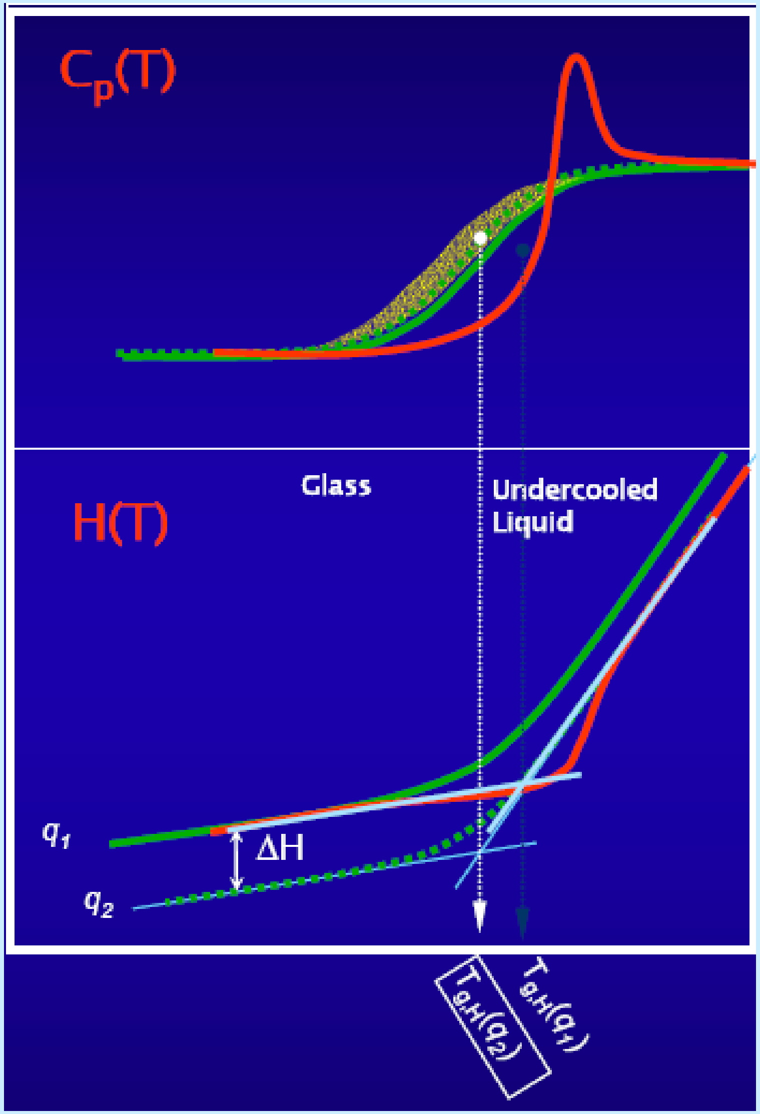

At a cooling rate *q1 > q2*: thermodynamic glass transition temperature Tg,H(*q1*) > Tg,H(*q2*)

Technologies of production of BMG

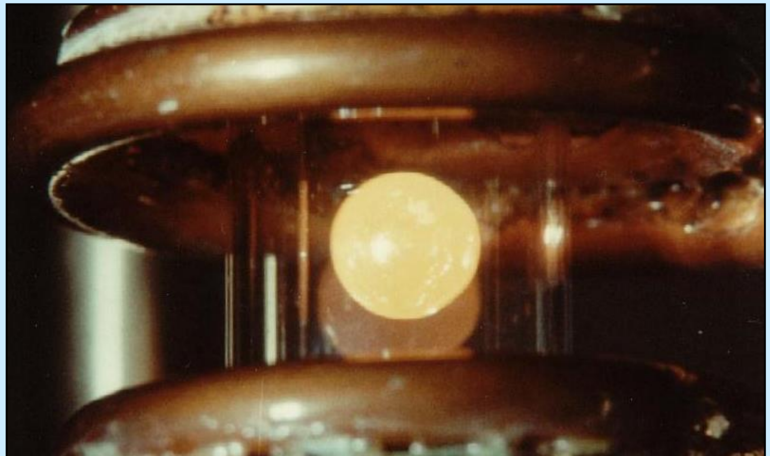

Levitation melting

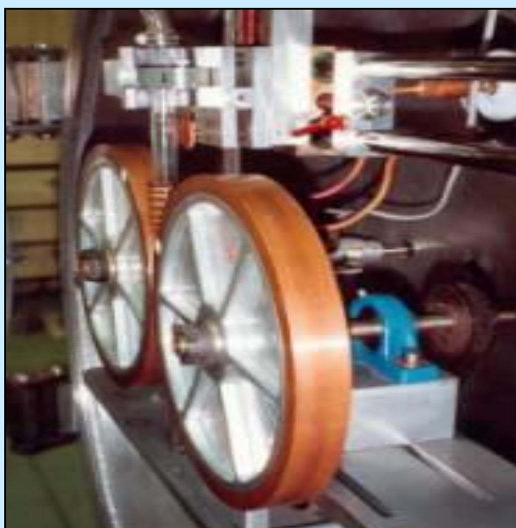

ribbons, thickness: 0,1~1mm

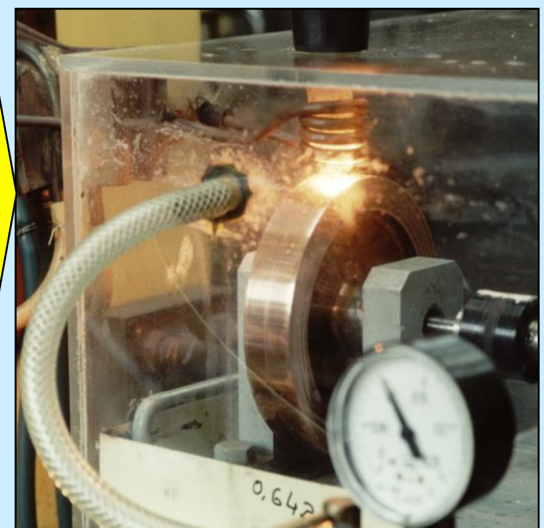

ribbons,thickness: ~ 50 μm

„first amorphous alloy”: AuSi - 1960

W. Clement, R.H. Willens and P. Duwez, Nature 187 (1960) 869

„first bulk metallic glass”: PdNi(P, Si) - 1984

H.W. Kui, A.L.Greer, D.Turnbull, Appl. Phys. Letters, 45(1984)615

„next metallic glasses” : MgLnM (M = Ni, Cu, Zn) – 1988

LaAl(TM) – 1989

Zr-based – 1990

Tohoku University – A. Inue

ZrTiCuNiBe (Vitreloy 1) – 1990

CalTec – W.L.Johnson

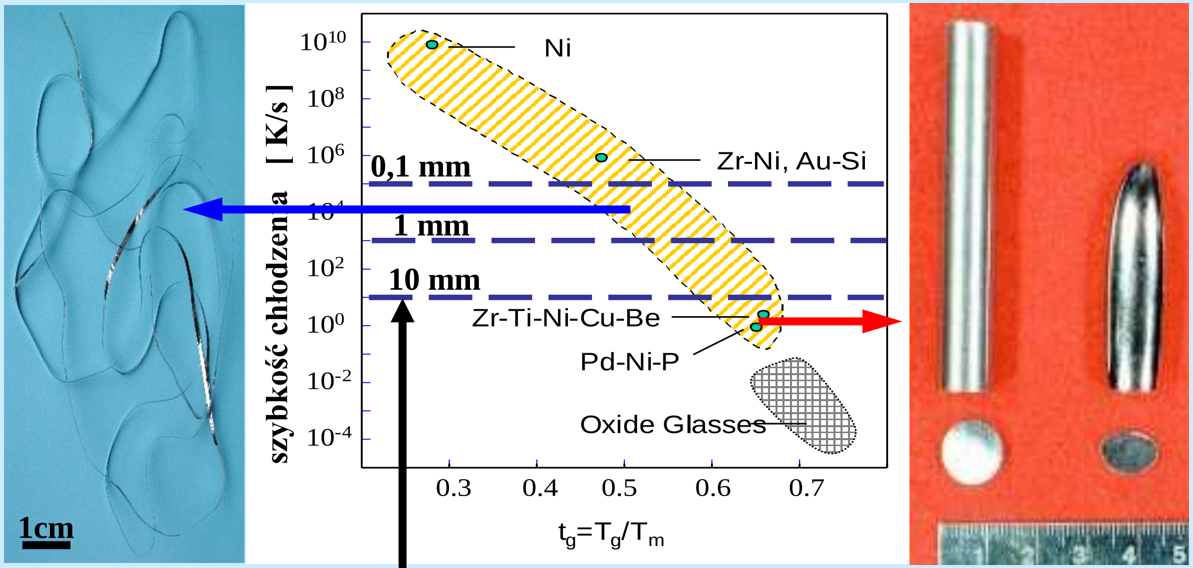

ϕ max producing amorphous material

(masywne szkło metaliczne ⇔ grubość ≥ 1mm)

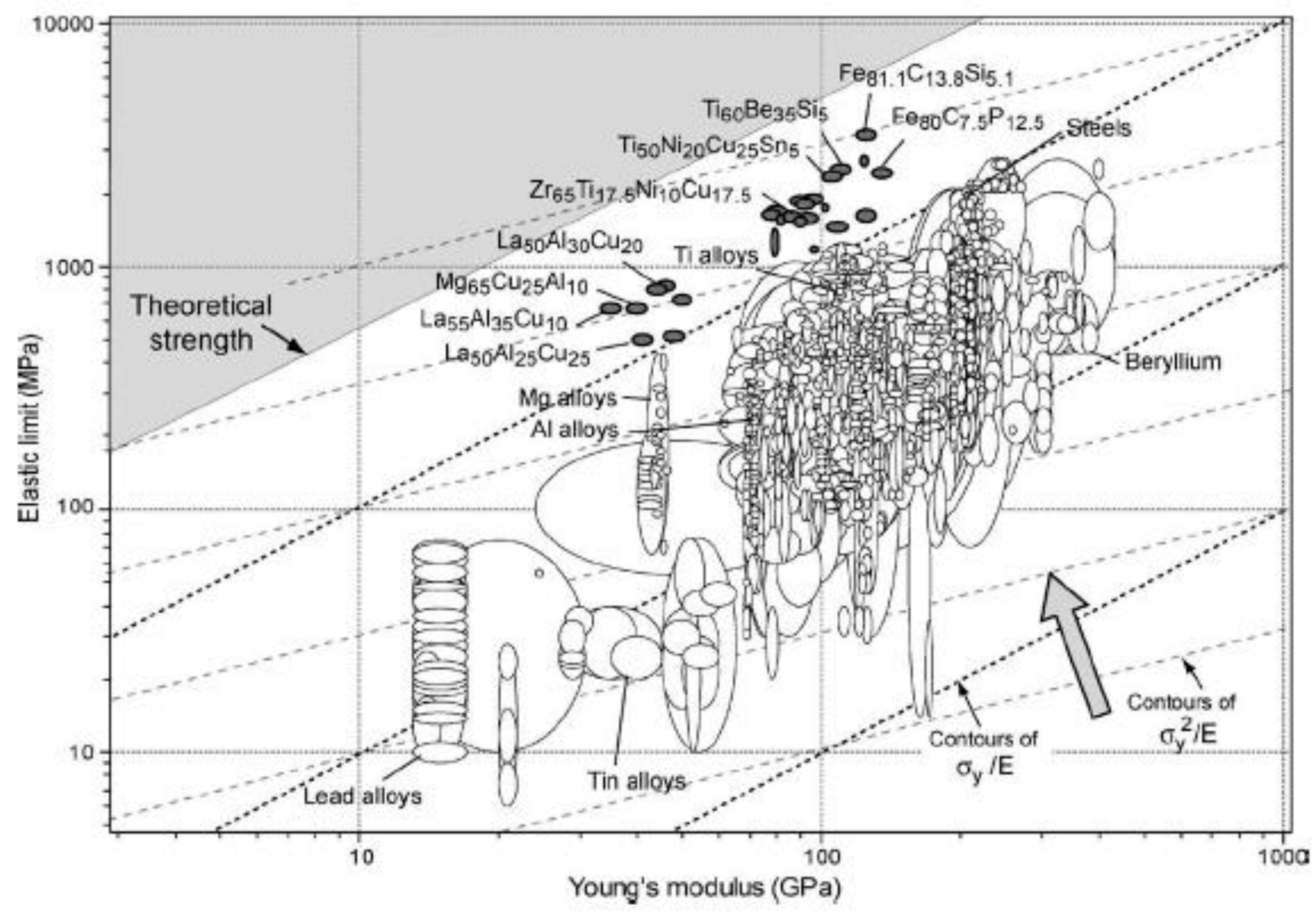

Elastic limit σ_y plotted against modulus E for 1507 metals, alloys, metal matrix composites and metallic glasses. The contours show the yield strain σ_y /E and the resilience σ^2/E.

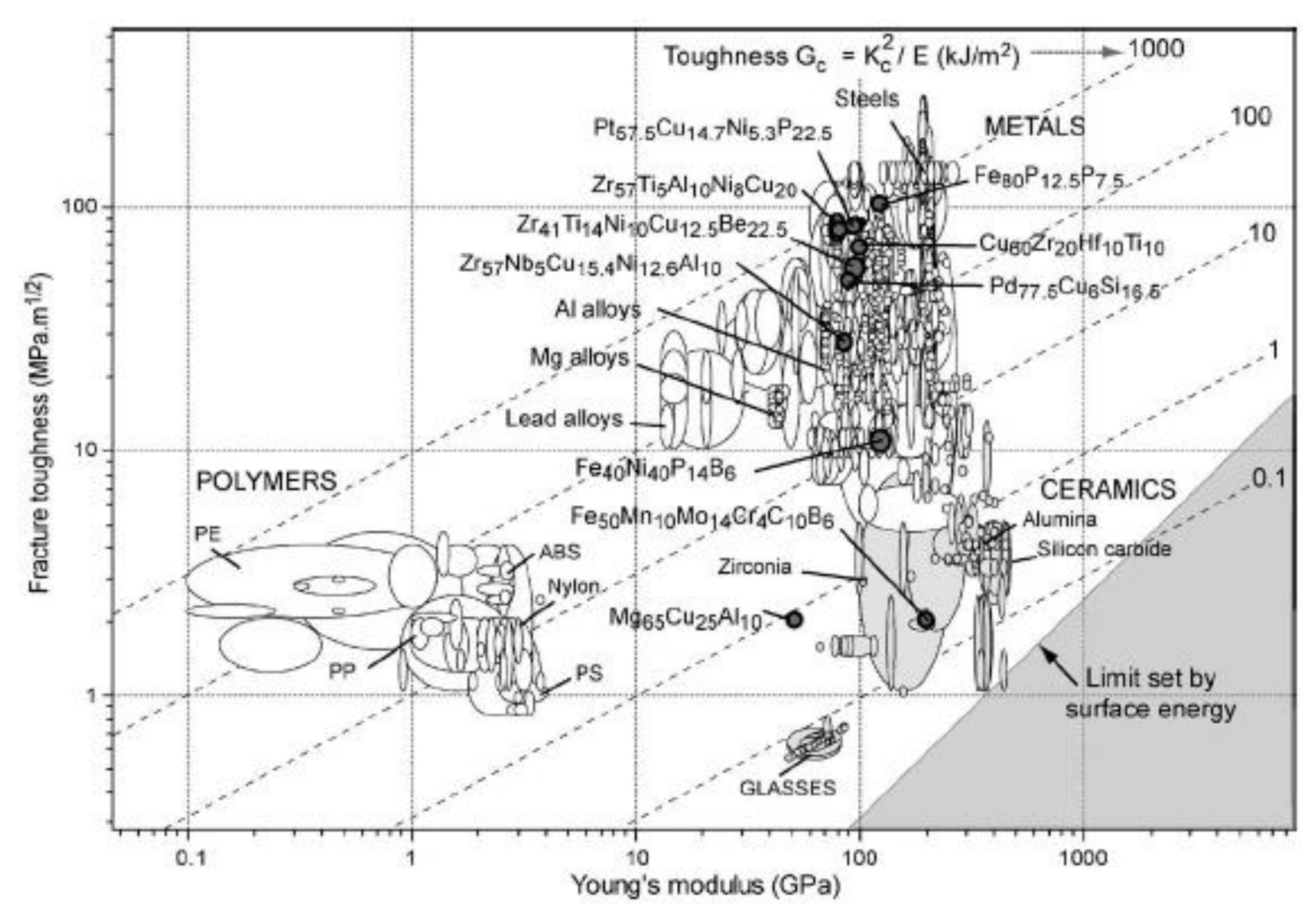

Fracture toughness and modulus for metals, alloys, ceramic, glasses, polymers and metallic glasses. The contours show the toughness G_c in kJm^{-2}.

Effect of alloying (negative enthalpy of mixing):
- reduction of melting point (formation of eutectics)
- ease of glass formation

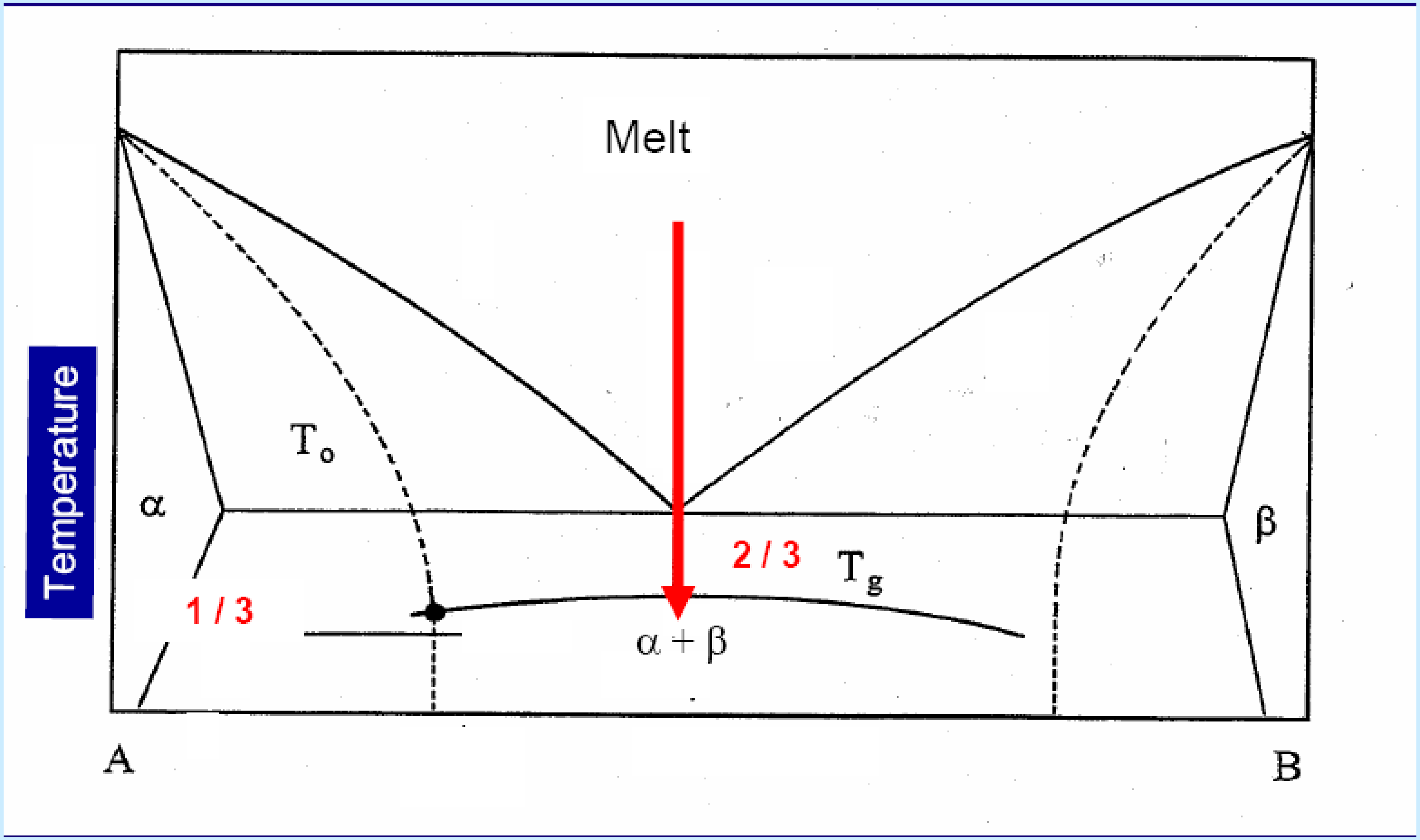

Composition dependence: $T_{liquidus}$ large, T_g small, Good glass former: T_g / $T_{m, element}$ ~ 1 / 3; T_g / T_{eut} ~ 2 / 3;

Early-Late Transition Metal

Metal-Metalloid

Glass forming ability of metallic alloys

Multi-component alloys (confusion principle)

Large difference in atomic radii > 12% (elastic energy)

Large negative enthalpy of mixing

Low eutectic temperature

High reduced glass transition temperature Tg / T_E

Avoid liquid / liquid phase separation

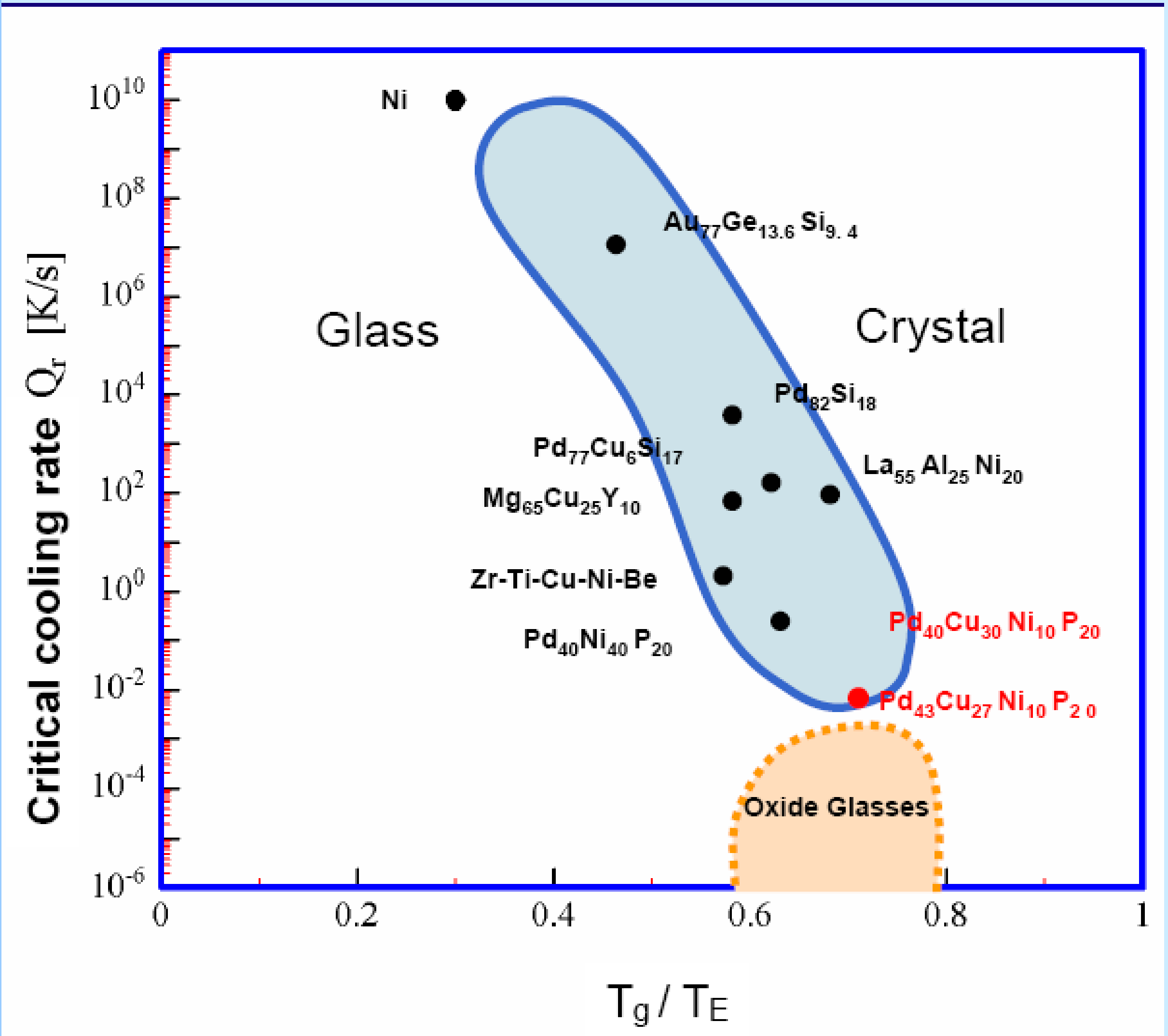

Kinetic control for (metallic) glass formation

Nucleation Control

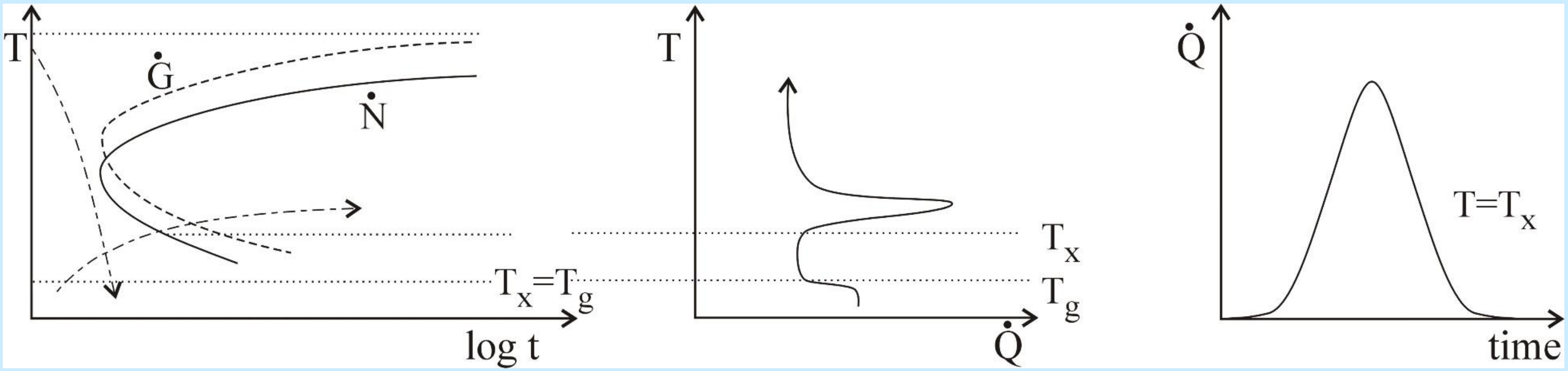

Growth Control

Kinetic balance to tune microstructure development !

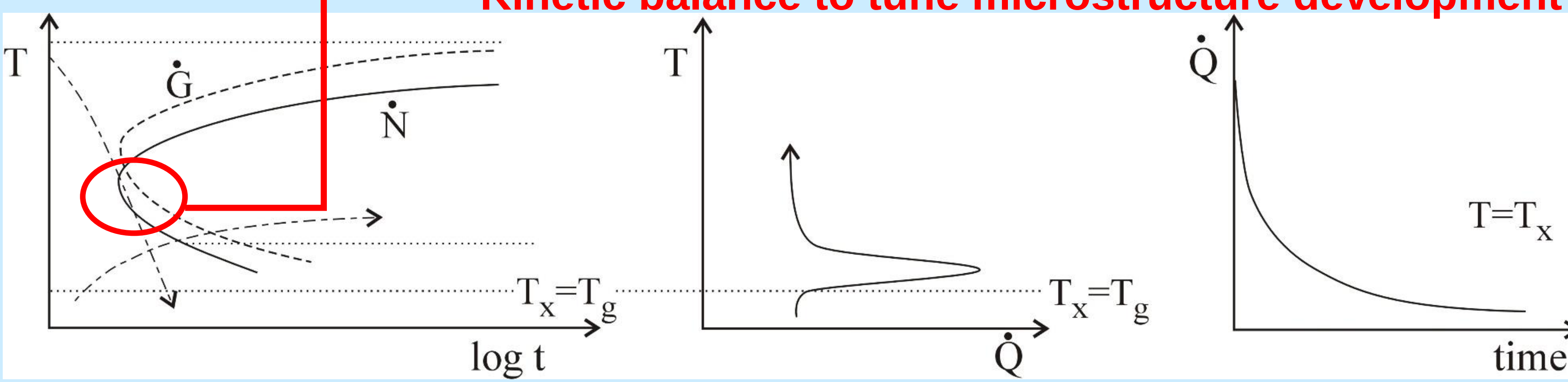

Thermal Stability

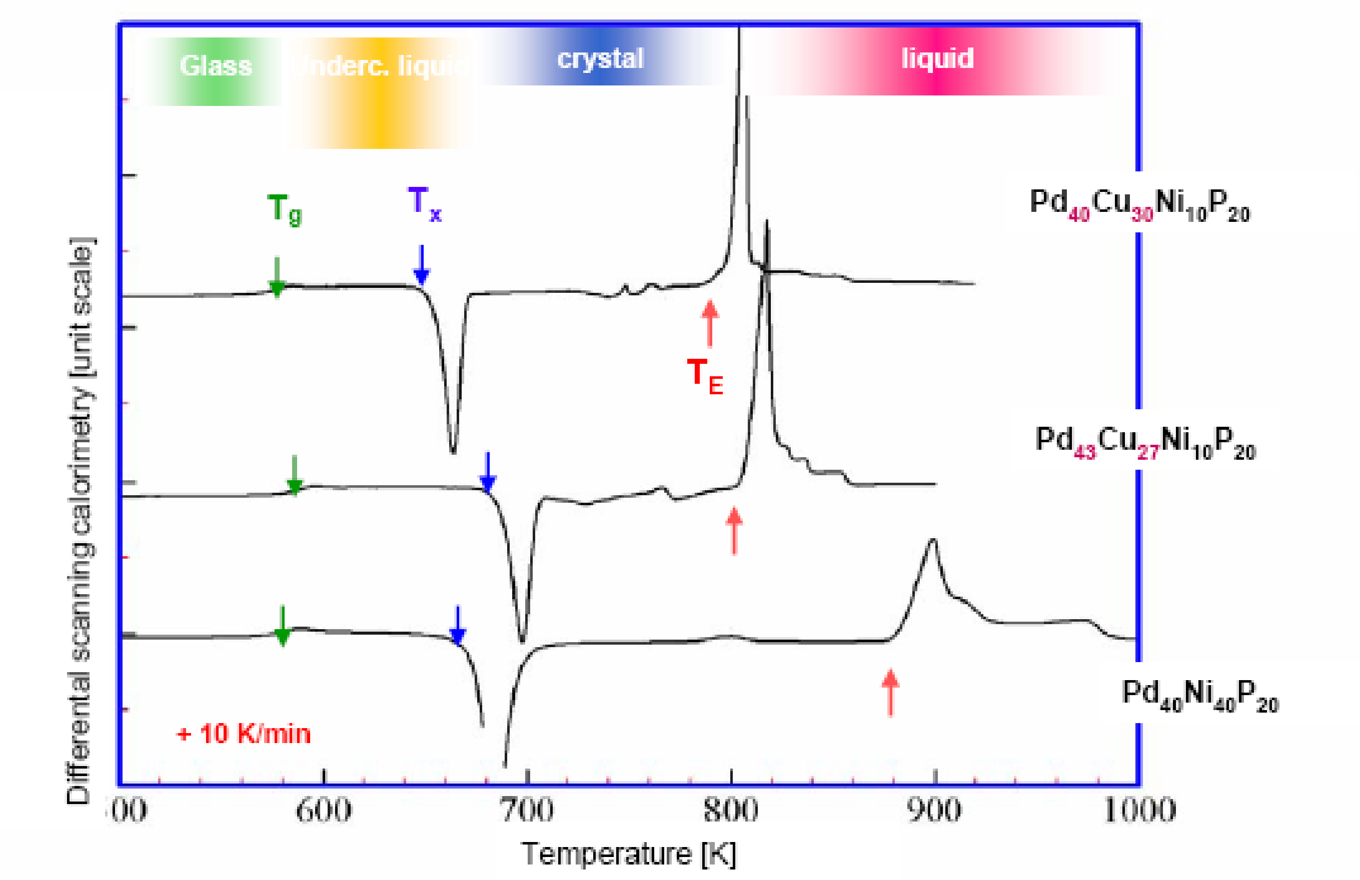

	$Pd_{40}Cu_{30}Ni_{10}P_{20}$	$Pd_{43}Cu_{27}Ni_{10}P_{20}$	$Pd_{40}Ni_{40}P_{20}$
Glass trans. temperature T_g *[K]*	*564*	*571*	*568*
Start of crystallization T_x *[K]*	*650*	*681*	*665*
Eutectic temperature T_E *[K]*	*798*	*802*	*884*
Enth. of fusion H_m *[kJ/ mol]*	*6.82*	*7.01*	*10.42*
T_g/ T_E	*0.71*	*0.71*	*0.64*

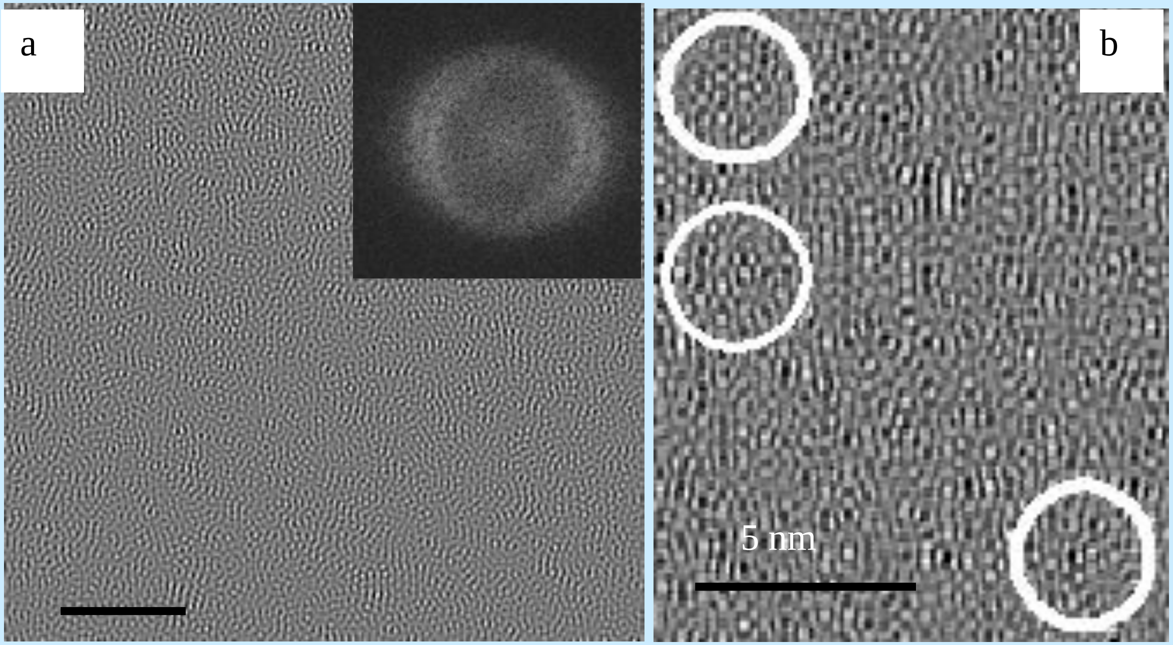

HREM (a), its Fourier transform as an insert in the corner, and two fragments after reverse Fourier transfer of the alloy Cu29Ni29Ti25Zr17 (G1C) after melt spinning at 20 m/s

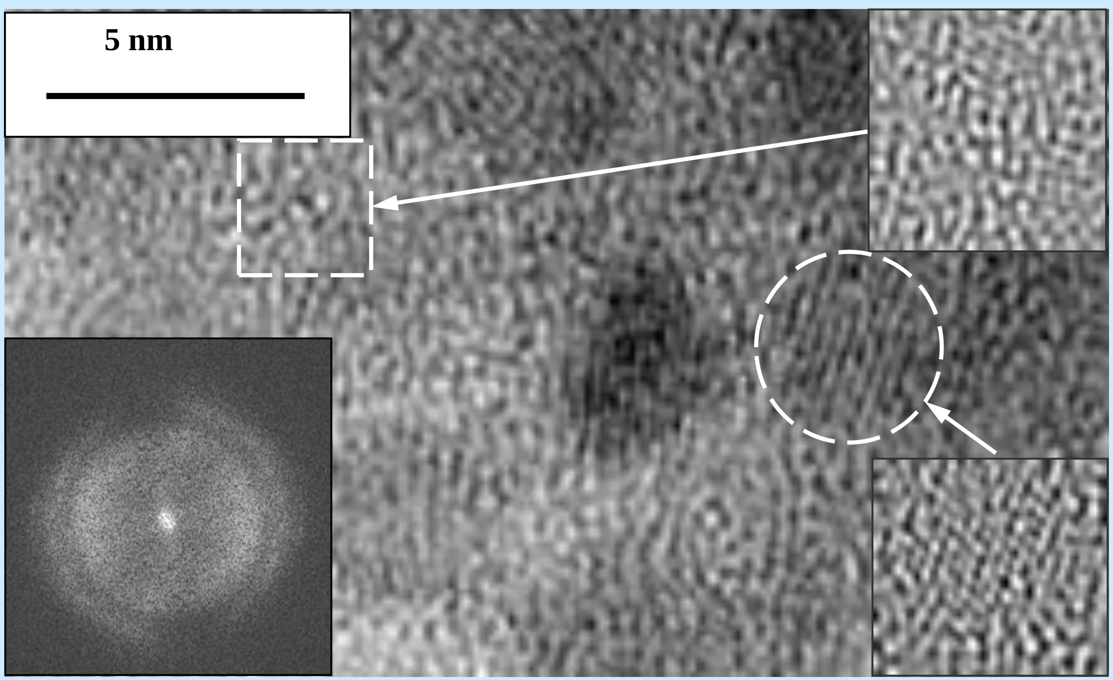

HREM (a), its Fourier transform as an insert in the corner, and reverse Fourier transform (b) of Cu25Ni25Ti25Zr25 (G0) after melt spinning at 10 m/s

Mechanical properties of Bulk Metallic Glasses (BMG)

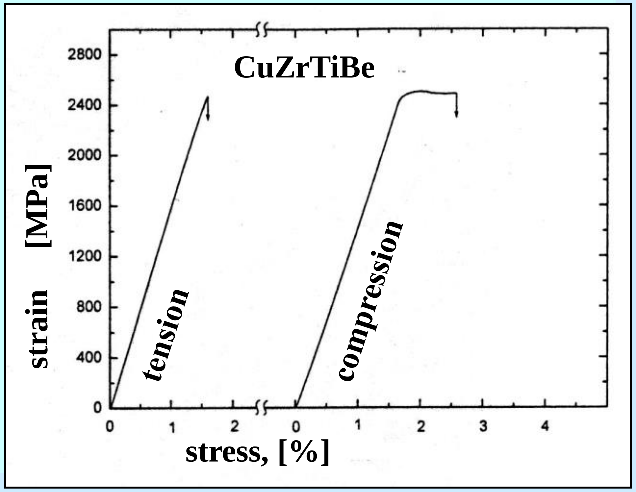

„Ashby charts”

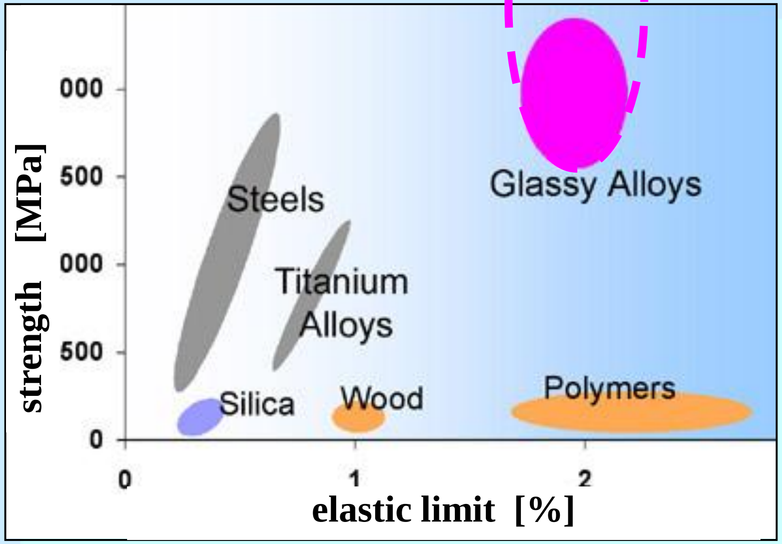

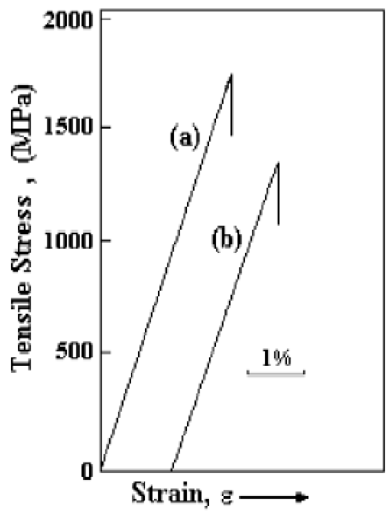

Fig. 4. Tensile stress–strain curves of the cast bulk metallic glasses. (a) $Zr_{52.5}Al_{10}Ni_{10}Cu_{15}Be_{12.5}$; (b) $Zr_{65}Al_{10}Ni_{10}Cu_{15}$.

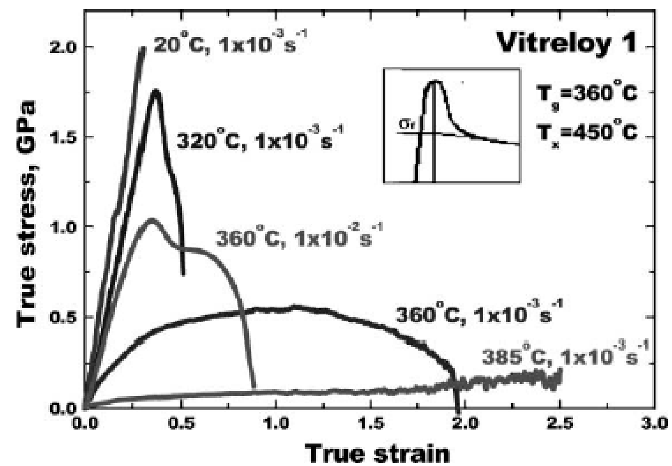

Fig. 4. True stress–true strain curves at $T < T_x$.

X. Xiao et al. / Journal of Alloys and Compounds 351 (2003) 324–328

$Zr_{41.2}Ti_{13.8}Cu_{12.5}Ni_{10}Be_{22.5}$ alloy (Vitreloy 1).

A.V. Sergueeva et al. / Journal of Non-Crystalline Solids 317 (2003) 169–175

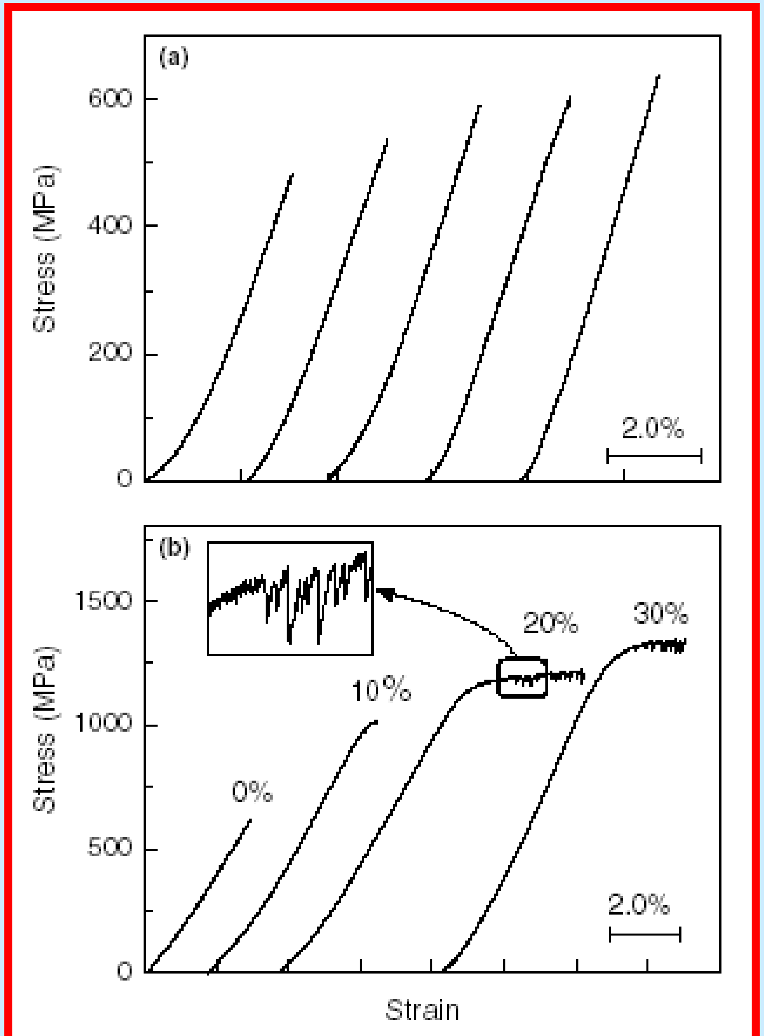

Mg65Cu25Y10 (a)
composite Mg65Cu25Y10+TiB (b)

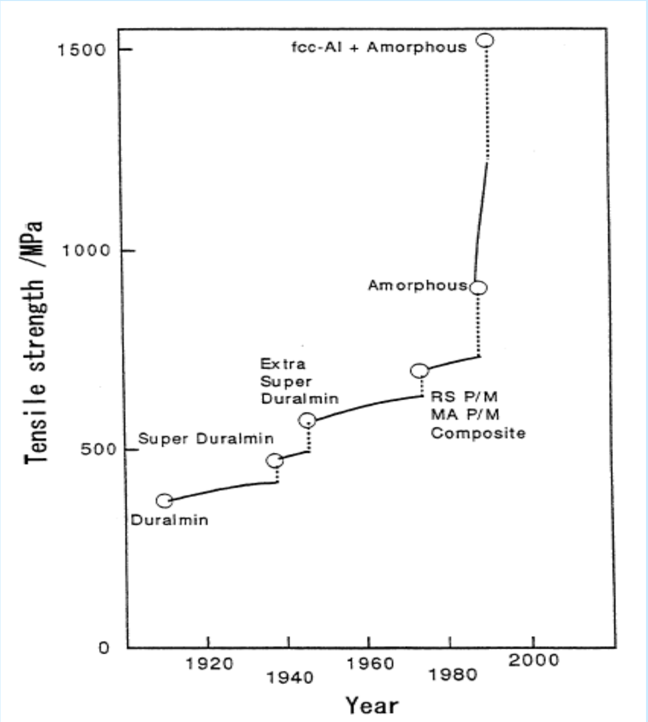

(Kim Y. H., Inoue A., Masumoto)

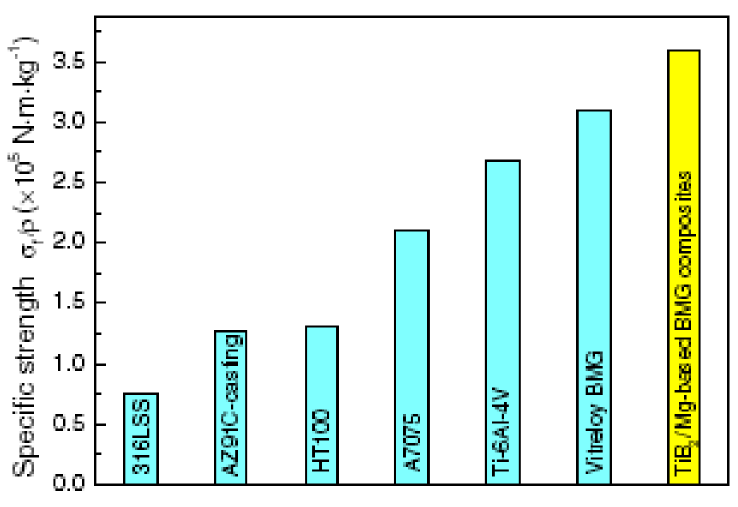

Plastic deformation of a thin plate of a thin plate of $Pd_{77.5}Cu_6Si_{16.5}$ glass in tension. **Shear bands** are consistent with **work-softening**.

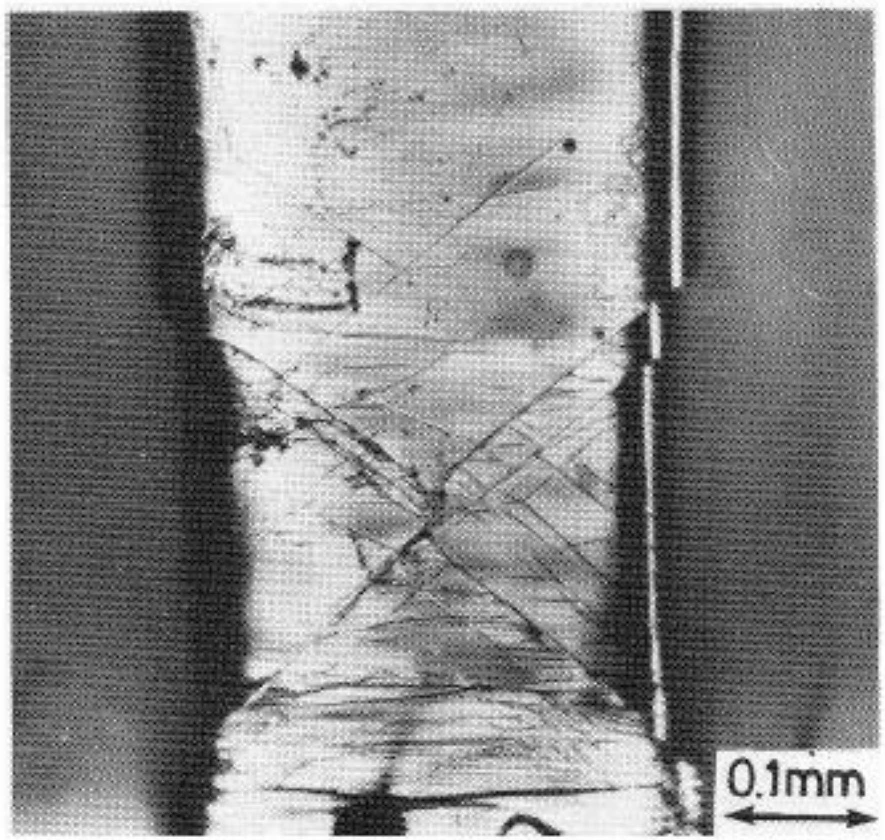

H. Kimura, PhD Thesis (1978) Tohoku Univ.